

A Mathematical Model Analysis of COVID-19 Transmission with Vaccination in Caputo Fractional Derivatives: Case Study in Indonesia

Muhammad Rifki Nisardi^{1*}, Kasbawati², Khaeruddin²

¹Department of Metallurgical Engineering, Institut Teknologi Bacharuddin Jusuf Habibie, Indonesia

²Department of Mathematics, Universitas Hasanuddin, Indonesia

muhammadrifkinisardi@ith.ac.id

ABSTRACT

Article History:

Received : 21-06-2024

Revised : 17-09-2024

Accepted : 11-10-2024

Online : 15-10-2024

Keywords:

SEIAR-V Model;
COVID-19 Model;
Basic Reproduction
Number;
Fractional Model;
Grunwald-Letnikov
Method.



This study aims to investigate a fractional-order mathematical model of COVID-19 transmission using the Caputo derivative definition which suitable to epidemiological cases by its advantage to explain memory effects. The model incorporates compartments for asymptomatic infections and includes a vaccination strategy aimed at mitigating the spread of COVID-19. We derived the disease-free and endemic equilibrium points for the fractional model and computed the basic reproduction number (R_0) using the Next-generation Matrix method. Additionally, we conducted sensitivity analyses of parameters affecting R_0 . The stability of the fractional model requires specific conditions to be met by the model parameters. To approximate active COVID-19 cases in Indonesia, we utilized the Explicit Grunwald-Letnikov method which well fit with Caputo fractional differential system. Simulation results demonstrate that the fractional-order model offers a flexible approach for modelling active COVID-19 cases in these regions. We found that fractional order for active cases COVID-19 in Indonesia is $\alpha = 0.9856$. The simulation showed that decreasing the vaccination rate and the efficacy of the vaccine would affect the reduction of COVID-19 transmission.



<https://doi.org/10.31764/jtam.v8i4.24711>



This is an open access article under the [CC-BY-SA](https://creativecommons.org/licenses/by-sa/4.0/) license

A. INTRODUCTION

Mathematical models of COVID-19 have garnered significant interest from researchers aiming to understand the mechanisms of its spread among people (Aldila et al., 2020; Annas et al., 2020; Iboi et al., 2020; Mwalili et al., 2020). Essentially, the mathematical models used to describe the dynamics of disease transmission are extensions of the basic SIR (Susceptible, Infected, and Recovered) and SEIR (Susceptible, Exposed, Infected, and Recovered) model. In some disease cases, the model is further developed by expanding the subpopulation categories considered. One such development involves incorporating the asymptomatic (A) subpopulation, resulting in the SEIAR model. Additionally, the inclusion of parameters such as quarantine, social distancing, and vaccination is applied to examine the effects of these parameter changes on the spread of a disease within a population.

Chávez et al. (2017) employed the SIR model and investigated Dengue transmission due to seasonal effects. Moreover, Aldila et al. (2020), the authors focused on social distancing and

rapid testing. They employed the SEIAR model and modified the asymptomatic compartment into two subclasses: asymptomatic undetected and asymptomatic detected.

Most models employ classical approaches to describe the dynamics of disease transmission. Classical models operate using differential and integral operators as defined in calculus studies. Numerous studies have demonstrated that classical models effectively explain the behaviour and spread of various types of diseases. However, in some cases, classical models have limitations that prevent them from capturing phenomena occurring in the dynamics of disease spread within a population. This phenomenon is referred to as the memory effect (Barros et al., 2021; Rihan, 2013). The memory effect is a phenomenon where a current outcome is influenced not only by present events but also by past events (memory). One common type of memory effect in epidemiology is hysteresis. In the case of hysteresis, the current events within a system are influenced not only by the present conditions but also by the conditions that occurred in the past.

The hysteresis occurs within an individual's self-defence mechanism when attacked by a disease. The self-defence mechanism is a critical factor in disease spread. The hysteresis effect provides the body with a memory of information related to the disease, enabling the body to recognize and combat the pathogen more effectively upon re-infection. Studies have shown that the memory effect observed in epidemiological issues can be explained using fractional mathematical models (Pimenov et al., 2012). As is well known, fractional calculus and fractional differential equations have recently been studied in various fields, including mathematics, physics, engineering, epidemiology, and other applied sciences (Bas et al., 2019; Gómez-Aguilar et al., 2013; Müller et al., 2011; Ndaïrou et al., 2021; Ozalp & Demirci, 2011; Saad, 2021; Tang, 2020). In line with the focus of this work, fractional mathematical models have been effectively used to describe the spread of COVID-19 cases in Wuhan, Spain, and Portugal, as proposed in (Ndaïrou et al., 2021). For each country, the fractional model provided a better approximation to real data with different values of the fractional order in Spain $\alpha = 0.85$, Portugal $\alpha = 0.75$.

We propose a modified SEIAR mathematical model of COVID-19 by incorporating vaccination and the fractional order in the Caputo derivative. We compute the disease-free equilibrium and endemic equilibrium. Additionally, we study the local stability of the equilibrium points and determine the basic reproduction number (R_0). We provide parameter estimation using '*fmincon*' optimization tools in MATLAB which based on real data of COVID-19 cases in Indonesia.

B. METHODS

In this section, we present the formulation of a COVID-19 spread model. The model development incorporates a vaccination scheme to account for active immunity in individuals, aiming to reduce the spread of COVID-19. This study also aims to develop a mathematical model using fractional calculus to analyse the effects of fractional order and vaccination on the spread of COVID-19. To achieve these objectives, we construct a model dividing the total population into six compartments: $S_u(t)$ represents the number of unvaccinated susceptible individuals at time t ; $S_v(t)$ denotes the number of vaccinated individuals at time t ; $E(t)$ represents the number of exposed individuals at time t ; $A(t)$ represents the number of asymptomatic infected individuals at time t ; $I(t)$ represents the number of symptomatic infected individuals at time t ;

and $R(t)$ represents the number of recovered individuals at time t . The interactions between these compartments are illustrated in Figure 1. It is assumed that everyone in the system has the same probability of being infected by COVID-19 and that there is no migration into or out of the system, keeping the total population constant.

The number of unvaccinated susceptible S_u naturally increase by natural recruitment with the rate Λ individual/time unit. Number of unvaccinated susceptible decrease through some factors as follows. After vaccination, individual who get vaccinated moves out from this compartment to susceptible vaccinated S_v with the rate $\tilde{\theta}$ per time unit. The decrease of unvaccinated susceptible is also caused from natural death process with rate $\tilde{\mu}$ per time unit. As we know, the COVID-19 can infect by human-to-human transmission. It assumed that the susceptible human can be infected by COVID-19 when they are in contact with individual who is being infected with symptoms or without symptoms. After it occurs, the susceptible unvaccinated will move to the exposed compartment with rate $\tilde{\beta}\phi S_u \frac{I}{N}$ and $\tilde{\beta}S_u \frac{A}{N}$ where $\tilde{\beta}$ per individual time unit is human to human transmission rate. ϕ is proportion of infected individual can spread the COVID-19 to susceptible humans.

Number of vaccinated susceptible S_v increase when unvaccinated individual being vaccinated. When someone gets a vaccination, it assumed that they may be still infected COVID-19 but the risk of human-to human transmission decrease by $(1 - \varepsilon)$, where ε is efficacy of vaccine. The high efficacy of vaccine will decrease the transmission of infected people to susceptible. So that, the number of vaccinated susceptible decrease when it moves out into exposed compartment after having a contact to infected people with rate $\tilde{\beta}\phi(1 - \varepsilon)S_u \frac{I}{N}$ and $\tilde{\beta}(1 - \varepsilon)S_u \frac{A}{N}$. Vaccinated susceptible also decrease by natural death with rate $\tilde{\mu}$ per time unit.

Number of exposed people (E) increase when people with infectious have a contact with unvaccinated susceptible and vaccinated susceptible. In this phase, it assumed that individual is in incubation period. The virus is in progress to infect human before it shows the symptoms or not. So that, exposed individual cannot infect others yet. Number of exposed people decrease by death rate $\tilde{\mu}$ and individual who move into symptomatic infectious I when they have symptoms of COVID-19 and into asymptomatic infectious A when they get no symptom after the incubation period with rate $\tilde{\sigma}$ per time unit.

The infectious compartment is divided into two subclasses, symptomatic (I) and asymptomatic infectious (A). When exposed people complete the incubation period and show the symptoms of COVID-19 such as fever, cough, or other mild symptoms then they move to symptomatic infectious (I), but when they have no symptoms then they move to asymptomatic infectious (A). Symptomatic or asymptomatic individual increase by people that move from exposed to infectious with rate $\tilde{\sigma}$ but in different proportion. p is denoted as proportion of exposed individuals who have progressed into Asymptomatic individual and $(1 - p)$ is proportion of exposed individuals who have progressed into symptomatic individual. These two compartments decrease by natural death $\tilde{\mu}$, \tilde{d} is the death rate caused by COVID-19 and movement to recovered population by recovery rate $\tilde{\gamma}_1$ and $\tilde{\gamma}_2$ respectively per time unit. Recovered individual R is people who test negative COVID-19 after being infectious. Recovered individual increase by recovered individual from asymptomatic infectious and symptomatic infectious. Recovered population decrease by natural death with rate $\tilde{\mu}$, as shown in Figure 1.

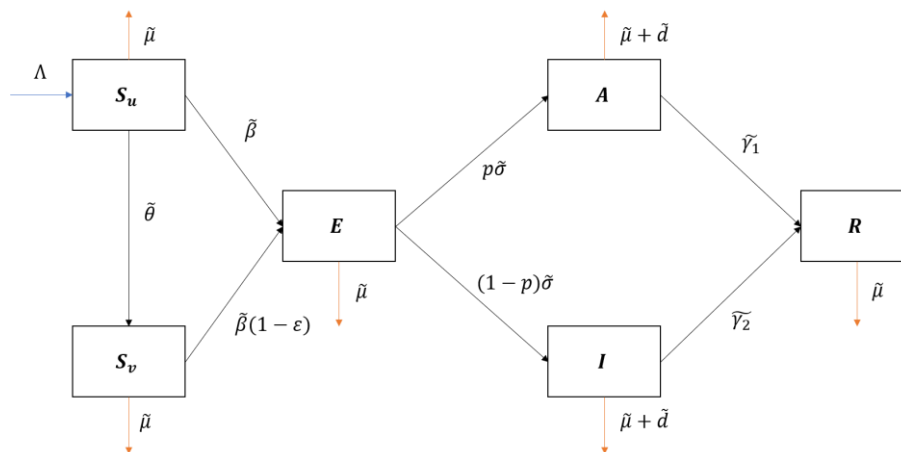


Figure 1. Transmission diagram of COVID-19 spread considering vaccination

Using diagram in Figure 1 and the assumption, the model of COVID-19 spread considering vaccination is expressed as the following equation.

$$\begin{aligned}
 \frac{dS_u}{dt} &= \tilde{\mu}N - \tilde{\mu}S_u - \tilde{\theta}S_u - \tilde{\beta}S_u \frac{\phi I}{N} - \tilde{\beta}S_u \frac{A}{N}, \\
 \frac{dS_v}{dt} &= \tilde{\theta}S_u - \tilde{\mu}S_v - \tilde{\beta}(1 - \epsilon)S_v \frac{\phi I}{N} - \tilde{\beta}(1 - \epsilon)S_v \frac{A}{N}, \\
 \frac{dE}{dt} &= \tilde{\beta}S_u \frac{\phi I}{N} + \tilde{\beta}S_u \frac{A}{N} + \tilde{\beta}(1 - \epsilon)S_v \frac{\phi I}{N} + \tilde{\beta}(1 - \epsilon)S_v \frac{A}{N} - \tilde{\mu}E - \tilde{\sigma}E, \\
 \frac{dA}{dt} &= p\tilde{\sigma}E - (\tilde{\mu} + \tilde{d})A - \tilde{\gamma}_1A, \\
 \frac{dI}{dt} &= (1 - p)\tilde{\sigma}E - (\tilde{\mu} + \tilde{d})I - \tilde{\gamma}_2I, \\
 \frac{dR}{dt} &= \tilde{\gamma}_2I + \tilde{\gamma}_1A - \tilde{d}R.
 \end{aligned} \tag{1}$$

Here N is total human population. Initial value for each variable is assumed as follow:

$$S_u(0) = S_{u0}, S_v(0) = S_{v0}, E(0) = E_0, A(0) = A_0, I(0) = I_0, R(0) = R_0,$$

where $S_{u0}, S_{v0}, E_0, A_0, I_0, R_0 \geq 0$. We assume that all parameters are positive. The parameters in model (1) are described in Table 1.

Table 1. Parameter in Model $S_u S_v EIAR$ COVID-19 in model (1).

Parameters	Description
$\tilde{\theta}$	Vaccination Rate
$\tilde{\beta}$	Contact transmission rate
ϕ	The proportion of symptomatic individuals transmitting the disease to susceptible individuals ($0 \leq \phi \leq 1$)
$\tilde{\mu}$	Natural birth rate/natural death rate
ε	Vaccine efficacy COVID-19 ($0 \leq \varepsilon \leq 1$)
$\tilde{\sigma}$	Incubation period from E to I
\tilde{d}	Death rate caused by COVID-19
p	The proportion of exposed individuals who are asymptotically infected ($0 \leq p \leq 1$)
$\tilde{\gamma}_1$	Recovery rate of asymptomatic
$\tilde{\gamma}_2$	Recovery rate of symptomatic

System (1) is expressed by first order ordinary differential equation system. In our purpose, the derivative of (1) will be defined as fractional derivative of fractional order α . We use a Caputo fractional derivative. Let us recall the definition of Caputo derivative: For an absolute continuous function $f: [0, \infty) \rightarrow \mathbb{R}$ the Caputo fractional derivative for order $\alpha > 0$ is given by (Petráš, 2011).

$${}^c_0D_t^\alpha f(t) = \frac{1}{\Gamma(n - \alpha)} \int_0^t (t - x)^{n-\alpha-1} f^{(n)}(x) dx,$$

where $\alpha \in (n - 1, n), n \in \mathbb{N}$. System with integer order (1) is generalized using Caputo fractional order system. Since the left side of (1) use the fractional derivative which have dimension $time^{-\alpha}$ (Bernal et al., 2012; Carvalho & Moreira-Pinto, 2021), it may cause the dimensional inconsistency. Thus, we define adjustments for several parameters to provide the consistency of dimension as follow:

$$\mu = \tilde{\mu}^\alpha; \theta = \tilde{\theta}^\alpha; \beta = \tilde{\beta}^\alpha; \sigma = \tilde{\sigma}^\alpha; d = \tilde{d}^\alpha; \gamma_1 = \tilde{\gamma}_1^\alpha; \gamma_2 = \tilde{\gamma}_2^\alpha$$

Therefore, we get Caputo fractional order systems

$$\begin{aligned} {}^c_0D_t^\alpha S_u(t) &= \Lambda - \mu S_u - \theta S_u - \beta S_u \frac{\phi I}{N} - \beta S_u \frac{A}{N}, \\ {}^c_0D_t^\alpha S_v(t) &= \theta S_u - \mu S_v - \beta(1 - \varepsilon) S_v \frac{\phi I}{N} - \beta(1 - \varepsilon) S_v \frac{A}{N}, \\ {}^c_0D_t^\alpha E(t) &= \beta S_u \frac{\phi I}{N} + \beta S_u \frac{A}{N} + \beta(1 - \varepsilon) S_v \frac{\phi I}{N} + \beta(1 - \varepsilon) S_v \frac{A}{N} - \mu E - \sigma E, \\ {}^c_0D_t^\alpha A(t) &= p\sigma E - (\mu + d)A - \gamma_1 A, \\ {}^c_0D_t^\alpha I(t) &= (1 - p)\sigma E - (\mu + d)I - \gamma_2 I \\ {}^c_0D_t^\alpha R(t) &= \gamma_2 I + \gamma_1 A - \mu R. \end{aligned} \tag{2}$$

Theorem 1. All solution of fractional order system (2), which belong to \mathbb{R}_+^6 are uniformly bounded and non-negative.

Proof: By following the approach of (Belgaid et al., 2021), we define $N(t) = S_u(t) + S_v(t) + E(t) + I(t) + A(t) + R(t)$. Thus, we get

$$\begin{aligned} {}_0^c D_t^\alpha N(t) &= {}_0^c D_t^\alpha S_u(t) + {}_0^c D_t^\alpha S_v(t) + {}_0^c D_t^\alpha E(t) + {}_0^c D_t^\alpha A(t) + {}_0^c D_t^\alpha I(t) + {}_0^c D_t^\alpha R(t), \\ &= \Lambda - \mu N - d(I + A) \\ &\leq \Lambda - \mu N \end{aligned}$$

Using standard comparison theorem for fractional system [23] we achieve that

$$N(t) \leq \left(N(0) - \frac{\Lambda}{\mu}\right) E_\alpha(-\mu t^\alpha) + \frac{\Lambda}{\mu}$$

where E_α is Mittag-Leffler function. Since $E_\alpha(-\mu t^\alpha) \rightarrow 0$ for $t \rightarrow \infty$ (Choi et al., 2014), then $N(t) \leq \frac{\Lambda}{\mu}$. Therefore, all solution of fractional system (2) that belong in \mathbb{R}_+^6 are still in region K, where

$$K = \left\{ (S_u, S_v, E, A, I, R) \in \mathbb{R}_+^6 : N(t) \leq \frac{\Lambda}{\mu} \right\}.$$

Additionally, we show that solutions of systems (2) are non-negative. From the first equation of system (2) we have

$$\begin{aligned} {}_0^c D_t^\alpha S_u(t) &= \Lambda - \mu S_u - \theta S_u - \beta S_u \frac{\phi I}{N} - \beta S_u \frac{A}{N} \\ &\geq - \left[\mu + \theta + \beta \frac{\phi I}{N} + \beta \frac{A}{N} \right] S_u \\ &\geq - [\mu + \theta + \beta(1 + \phi)] S_u \\ &\geq -C_1 S_u \end{aligned}$$

with $C_1 = \mu + \theta + \beta(1 + \phi)$. According to standard comparison theorem for fractional order (Askar et al., 2021) and positivity properties of Mittag Leffler function (Belgaid et al., 2021).

$$S_u \geq S_u(0)E_\alpha(-C_1 t^\alpha) \Rightarrow S_u \geq 0.$$

Furthermore, we can prove all equations in System (2) are non-negative in the same way

$$\begin{aligned} S_v &\geq S_v(0)E_\alpha(-C_2 t^\alpha) \Rightarrow S_v \geq 0 \\ E &\geq E(0)E_\alpha(-C_3 t^\alpha) \Rightarrow E \geq 0. \\ A &\geq A(0)E_\alpha(-C_4 t^\alpha) \Rightarrow A \geq 0. \\ I &\geq I(0)E_\alpha(-C_5 t^\alpha) \Rightarrow I \geq 0. \\ R &\geq R(0)E_\alpha(-\mu t^\alpha) \Rightarrow R \geq 0. \end{aligned}$$

Where $C_2, C_3, C_4, C_5 \geq 0$. It has been proved the solution of systems (2) are non-negative. ■
 To simplify the model, we introduce some new dimensionless variables, i.e.

$$s_u(t) = \frac{S_u(t)}{N}, s_v(t) = \frac{S_v(t)}{N}, e(t) = \frac{E(t)}{N}, i(t) = \frac{I(t)}{N}, a(t) = \frac{A(t)}{N}, r(t) = \frac{R(t)}{N} \tag{3}$$

The variables (3) provide proportion of human population. If dimensionless variables (3) are substituted to (2) then we formulate a new model with dimensionless variable

$$\begin{aligned} {}_0^C D_t^\alpha s_u(t) &= \mu - \mu s_u - \theta s_u - \beta \phi s_u i - \beta s_u a, \\ {}_0^C D_t^\alpha s_v(t) &= \theta s_u - \mu s_v - \beta \phi (1 - \varepsilon) s_v i - \beta (1 - \varepsilon) s_v a, \\ {}_0^C D_t^\alpha e(t) &= \beta \phi s_u i + \beta s_u a + \beta \phi (1 - \varepsilon) s_v i + \beta (1 - \varepsilon) s_v a - \mu e - \sigma e, \\ {}_0^C D_t^\alpha a(t) &= p \sigma e - (\mu + d) a - \gamma_1 a, \\ {}_0^C D_t^\alpha i(t) &= (1 - p) \sigma e - (\mu + d) i - \gamma_2 i, \\ {}_0^C D_t^\alpha r(t) &= \gamma_2 i + \gamma_1 a - \mu r, \end{aligned} \tag{4}$$

where $s_u(0) = s_{u0}, s_v(0) = s_{v0}, e(0) = e_0, a(0) = a_0, i(0) = i_0, r(0) = r_0$.

C. RESULT AND DISCUSSION

1. Disease free and Endemic Equilibrium Point

The equilibrium of fractional model is obtained when (Choi et al., 2014; Keshtkar et al., 2014).

$${}_0^C D_t^\alpha (s_u) = 0, {}_0^C D_t^\alpha (s_v) = 0, {}_0^C D_t^\alpha (e) = 0, {}_0^C D_t^\alpha (a) = 0, {}_0^C D_t^\alpha (i) = 0, {}_0^C D_t^\alpha (r) = 0.$$

We obtained the disease free-equilibrium point of the model, i.e.

$$X_0 = (s_u, s_v, e, i, a, r) = \left(\frac{\mu}{\mu + \theta}, \frac{\theta}{\mu + \theta}, 0, 0, 0, 0 \right).$$

The Endemic equilibrium point occurs when $a \neq 0$ and $i \neq 0$. It means that there are infected individuals who can spread COVID-19 to others. Endemic point for systems (4) is expressed as:

$$X_1 = (s_u^*, s_v^*, e^*, a^*, i^*, r^*)$$

with

$$\begin{aligned} s_u^* &= \frac{\mu}{\mu + \theta + c_0 i^*}, \\ s_v^* &= \frac{\theta \mu}{(\mu + (1 - \varepsilon) c_0 i^*)(\mu + \theta + c_0 i^*)}, \\ e^* &= \frac{(\mu + d + \gamma_2)}{(1 - p) \sigma} i^*, \\ a^* &= \frac{p(\mu + d + \gamma_2)}{(1 - p)(\mu + d + \gamma_1)} i^*, \\ r^* &= \left(\frac{p \gamma_1 (\mu + d + \gamma_2) + (1 - p) \gamma_2 (\mu + d + \gamma_1)}{\mu (1 - p) (\mu + d + \gamma_1)} \right) i^*. \end{aligned}$$

$s_u^*, s_v^*, e^*, a^*, i^*, r^*$ expressed as a function of i^* , whereas i^* is taken from positive roots of the polynomial:

$$P(I) = Ai^{*3} + Bi^{*2} + Ci^* + D = 0,$$

with

$$\begin{aligned} A &= -v\delta c_0^2, \\ B &= \mu\delta c_0^2 - v(\mu\delta + \theta\delta + \mu)c_0, \\ C &= \mu^2 c_0 - v(\mu^2 + \mu\theta), \\ D &= \delta\mu\theta c_0. \end{aligned}$$

here $v = \frac{(\mu+\sigma)(\mu+d+\gamma_2)}{(1-p)\sigma}$, $\delta = (1 - \varepsilon)$, $c_0 = \frac{\beta((1-p)\phi(\mu+d+\gamma_1)+p(\mu+d+\gamma_2))}{(1-p)(\mu+d+\gamma_1)}$.

2. Basic Reproduction Number and Sensitivity Analysis

Basic reproduction number (R_0) can be determined using the next-generation matrix approach (Keshtkar et al., 2014). Let

$$F = \begin{pmatrix} 0 & \beta s_u + \beta(1 - \varepsilon)s_v & \beta\phi s_u + \beta\phi(1 - \varepsilon)s_v \\ 0 & 0 & 0 \\ 0 & 0 & 0 \end{pmatrix},$$

and

$$V = \begin{pmatrix} \mu + \sigma & 0 & 0 \\ -p\sigma & \mu + d + \gamma_1 & 0 \\ -(1-p)\sigma & 0 & \mu + d + \gamma_2 \end{pmatrix}.$$

Then we obtained

$$V^{-1} = \begin{pmatrix} \frac{1}{\mu + \sigma} & 0 & 0 \\ \frac{p\sigma}{(\mu + \sigma)(\mu + d + \gamma_1)} & \frac{1}{\mu + d + \gamma_1} & 0 \\ \frac{(1-p)\sigma}{(\mu + \sigma)(\mu + d + \gamma_2)} & 0 & \frac{1}{\mu + d + \gamma_2} \end{pmatrix},$$

and then,

$$FV^{-1} = \begin{bmatrix} \frac{\beta\rho\sigma\left(\frac{\mu + \theta\delta}{\mu + \theta}\right)}{(\mu + \sigma)(\mu + d + \gamma_1)} + \frac{\beta(1-p)\phi\sigma\left(\frac{\mu + \theta\delta}{\mu + \theta}\right)}{(\mu + \sigma)(\mu + d + \gamma_2)} & \frac{\beta\rho\sigma\left(\frac{\mu + \theta\delta}{\mu + \theta}\right)}{(\mu + d + \gamma_1)} & \frac{\beta\phi\rho\sigma\left(\frac{\mu + \theta\delta}{\mu + \theta}\right)}{(\mu + d + \gamma_2)} \\ 0 & 0 & 0 \\ 0 & 0 & 0 \end{bmatrix}.$$

Thus, using matrix generation method, we found:

$$R_0 = \frac{\beta\sigma(\mu + \theta\delta)}{(\mu + \theta)(\mu + \sigma)} \left(\frac{p}{\mu + d + \gamma_1} + \frac{(1-p)\phi}{\mu + d + \gamma_2} \right). \tag{5}$$

The objective of conducting sensitivity analysis on the basic reproduction number is to assess the significance of each parameter in disease transmission. This analysis employs the

normalized sensitivity index of a variable with respect to a particular parameter, defined as the ratio of the relative change in the variable to the relative change in the parameter. When the variable is differentiable with respect to the parameter, the sensitivity index can be formally defined as follows.

- a. The sensitivity analysis R_0 with respect to θ

$$C_{\theta}^{R_0} = \frac{\partial R_0}{\partial \theta} \times \frac{\theta}{R_0} = \frac{-\varepsilon \theta d}{(d + \sigma)(d + \theta)(d + (1 - \varepsilon)\theta)} < 0$$

The sensitivity analysis of R_0 with respect to θ illustrates the relationship between the vaccination rate of susceptible and the change in the basic reproduction number. Since all parameters are positive, the analysis indicates a negative value, signifying an inverse relationship. Thus, as the parameter θ , representing the vaccination rate, increases, the value of R_0 decreases. For details, see Appendix A.1.

- b. The sensitivity analysis R_0 with respect to ε

$$C_{\varepsilon}^{R_0} = \frac{\partial R_0}{\partial \varepsilon} \times \frac{\varepsilon}{R_0} = \frac{-\theta \varepsilon}{d + \theta(1 - \varepsilon)} < 0$$

Similarly, to the previous finding, the sensitivity analysis of R_0 with respect to ε yields a negative value. This indicates that a higher efficacy rate of the vaccine results in a decrease in R_0 . Therefore, R_0 is contingent upon the effectiveness of the vaccine. For details, see Appendix A.2.

3. Local Stability of Equilibrium Point

- a. Local Stability of COVID-19 Free Equilibrium Point

The stability of DFE point can be analysed by linearization involving Jacobian matrix. From the system (4) we obtain the Jacobian matrix and evaluate it in DFE point. Thus, we get

$$J(X_0) = \begin{pmatrix} -\psi & 0 & 0 & -\kappa_1 & -\kappa_1 \phi & 0 \\ \theta & -\mu & 0 & -\kappa_2 & -\kappa_2 \phi & 0 \\ 0 & 0 & -\kappa_3 & \kappa_1 + \kappa_2 & (\kappa_1 + \kappa_2) \phi & 0 \\ 0 & 0 & p\sigma & -\kappa_4 & 0 & 0 \\ 0 & 0 & (1 - p)\sigma & 0 & -\kappa_5 & 0 \\ 0 & 0 & 0 & \gamma_1 & \gamma_2 & -\mu \end{pmatrix} \tag{6}$$

with

$$\psi = \mu + \theta, \kappa_1 = \frac{\beta \mu}{\psi}, \kappa_2 = \beta \delta \frac{\theta}{\psi}, \kappa_3 = \mu + \sigma, \kappa_4 = \mu + d + \gamma_1, \kappa_5 = \mu + d + \gamma_2$$

We can obtain the eigen value by evaluating (6)

$$\det(\lambda I - J(X_0)) = 0$$

$$\det \begin{pmatrix} \lambda + \psi & 0 & 0 & -\kappa_1 & -\kappa_1\phi & 0 \\ \theta & \lambda + \mu & 0 & -\kappa_2 & -\kappa_2\phi & 0 \\ 0 & 0 & \lambda + \kappa_3 & \kappa_1 + \kappa_2 & (\kappa_1 + \kappa_2)\phi & 0 \\ 0 & 0 & p\sigma & \lambda + \kappa_4 & 0 & 0 \\ 0 & 0 & (1-p)\sigma & 0 & \lambda + \kappa_5 & 0 \\ 0 & 0 & 0 & \gamma_1 & \gamma_2 & \lambda + \mu \end{pmatrix} = 0 \tag{7}$$

or

$$(\lambda + \mu)^2(\lambda + \psi)(\lambda^3 + (\kappa_3 + \kappa_4 + \kappa_5)\lambda^2 + (\kappa_3\kappa_4 + \kappa_3\kappa_5 + \kappa_4\kappa_5 + ((-1 + p)\phi - p)(\kappa_1 + \kappa_2)\sigma)\lambda + \kappa_3\kappa_4\kappa_5 + (\kappa_1 + \kappa_2)(p\kappa_5 + (1 - p)\phi\kappa_4)\sigma) = 0$$

From characteristic polynomial, we obtain the eigen value $\lambda_{1,2} = -\mu, \lambda_3 = -(\mu + \theta)$. Because $\mu, \theta > 0$, so that $\lambda_{1,2,3} < 0$ or in the other hand $|\arg(\lambda_i)| = \pi$. Thus for $0 \leq \alpha < 1$, $|\arg(\lambda_{1,2,3})| > \frac{\alpha\pi}{2}$. The stability of equilibrium point depends on the third order polynomial

$$\lambda^3 + a_1\lambda^2 + a_2\lambda + a_3 = 0 \tag{8}$$

Where

$$a_1 = \kappa_3 + \kappa_4 + \kappa_5,$$

$$a_2 = \kappa_3\kappa_4 + \kappa_3\kappa_5 + \kappa_4\kappa_5 + ((-1 + p)\phi - p)(\kappa_1 + \kappa_2)\sigma$$

$$a_3 = \kappa_3\kappa_4\kappa_5 + (\kappa_1 + \kappa_2)(p\kappa_5 + (1 - p)\phi\kappa_4)\sigma = \kappa_3\kappa_4\kappa_5(1 - R_0).$$

The equation (8) will satisfy $|\arg(\lambda_i)| > \frac{\alpha\pi}{2}$ if one of these conditions hold

- For $D(p) > 0$ will be satisfied if $18a_1a_2a_3 + (a_1a_2)^2 > 4a_3a_2^3 + 27a_3^2$,
 - $a_1 > 0$
 - $a_3 > 0$
 - $a_1a_2 > a_3$.
- (9)

Because all parameters assumed positive, we have $a_1 = \kappa_3 + \kappa_4 + \kappa_5 > 0$ and $a_3 = \kappa_3\kappa_4\kappa_5(1 - R_0) > 0$ if $R_0 < 1$. Hence, we need to satisfy the condition $a_1a_2 > a_3$ so that based on (Ahmed et al., 2006) this following inequality $|\arg(\lambda_i)| > \frac{\alpha\pi}{2}$ is guaranteed for all $0 \leq \alpha < 1$. Therefore, disease free equilibrium X_0 is locally asymptotically stable near X_0 point.

- For $D(p) < 0$ will be satisfied that condition if
- $18a_1a_2a_3 + (a_1a_2)^2 < 4a_3a_2^3 + 27a_3^2$,

Stability of X_0 when $D(p) < 0$ can be obtained if one of these conditions hold

First stability condition (C-1)

- $a_1 \geq 0$,
- $a_2 \geq 0$,
- $a_3 > 0$.

Because all parameters assumed positive, we have $a_1 = \kappa_3 + \kappa_4 + \kappa_5 > 0$ and $a_3 = \kappa_3\kappa_4\kappa_5(1 - R_0) > 0$ if $R_0 < 1$. Hence, we need to satisfy the condition $\kappa_3\kappa_4 + \kappa_3\kappa_5 + \kappa_4\kappa_5 \geq ((1 - p)\varphi + p)(\kappa_1 + \kappa_2)\sigma$ to claim $a_2 \geq 0$. Based on (Ahmed et al., 2006) this following inequality $|\arg(\lambda_i)| > \frac{\alpha\pi}{2}$ is guaranteed for all $\alpha < \frac{2}{3}$. Therefore, disease free equilibrium X_0 is locally asymptotically stable near X_0 point.

Second stability condition (C-2)

- $a_1 > 0$
- $a_2 > 0$ and
- $a_1a_2 = a_3$.

We have $a_1 = \kappa_3 + \kappa_4 + \kappa_5 > 0$ and $a_2 \geq 0$ if $\kappa_3\kappa_4 + \kappa_3\kappa_5 + \kappa_4\kappa_5 \geq ((1 - p)\varphi + p)(\kappa_1 + \kappa_2)\sigma$. Hence, we need to satisfy $(\kappa_3 + \kappa_4 + \kappa_5)(\kappa_3\kappa_4 + \kappa_3\kappa_5 + \kappa_4\kappa_5 - ((1 - p)\varphi + p)(\kappa_1 + \kappa_2)\sigma) - \kappa_3\kappa_4\kappa_5(1 - R_0) = 0$ to claim $a_1a_2 = a_3$. this following inequality $|\arg(\lambda_i)| > \frac{\alpha\pi}{2}$ is guaranteed for all $0 \leq \alpha < 1$ s. Therefore, disease free equilibrium X_0 is locally asymptotically stable near X_0 point.

b. Local Stability of COVID-19 Endemic Equilibrium Point

The stability of endemic point can be analysed by linearization involving Jacobian matrix. From the system (4) we obtain the Jacobian matrix and evaluate it in endemic point. Thus, we get

$$J(X_1) = \begin{pmatrix} -\kappa_1 - \psi_1 & 0 & 0 & -\psi_3 & -\varphi\psi_3 & 0 \\ \theta & -\mu - \psi_2 & 0 & -\psi_4 & -\varphi\psi_4 & 0 \\ \psi_1 & \psi_2 & -\kappa_2 & \psi_3 + \psi_4 & \psi_3 + \psi_4 & 0 \\ 0 & 0 & p\sigma & -\kappa_3 & 0 & 0 \\ 0 & 0 & (1 - p)\sigma & 0 & -\kappa_4 & 0 \\ 0 & 0 & 0 & \gamma_1 & \gamma_2 & -\mu \end{pmatrix} \tag{10}$$

where

$$\psi_1 = \beta(\varphi i^* + a^*), \psi_2 = (1 - \varepsilon)\psi_1, \psi_3 = \beta s_u^*, \psi_4 = \beta(1 - \varepsilon)s_v^*, \kappa_1 = \mu + \theta, \kappa_2 = \mu + \sigma, \kappa_3 = \mu + d + \gamma_1, \kappa_4 = \mu + d + \gamma_2.$$

We can obtain the eigen value by evaluating (10)

$$\det(\lambda I - J(X_1)) = 0$$

$$\det \begin{pmatrix} \lambda + (\kappa_1 + \psi_1) & 0 & 0 & -\psi_3 & -\psi_3 & 0 \\ \theta & \lambda + (\mu + \psi_2) & 0 & -\psi_4 & -\psi_4 & 0 \\ \psi_1 & \psi_2 & \lambda + \kappa_2 & \psi_3 + \psi_4 & \psi_3 + \psi_4 & 0 \\ 0 & 0 & p\sigma & \lambda + \kappa_3 & 0 & 0 \\ 0 & 0 & (1-p)\sigma & 0 & \lambda + \kappa_4 & 0 \\ 0 & 0 & 0 & \gamma_1 & \gamma_2 & \lambda + \mu \end{pmatrix} = 0 \quad (11)$$

or

$$(\lambda + \mu)(\lambda^5 + b_1\lambda^4 + b_2\lambda^3 + b_3\lambda^2 + b_4\lambda + b_5) = 0,$$

with b_1, b_2, b_3, b_4, b_5 are coefficient of the fifth order polynomial. From characteristic polynomial, we obtain the eigen value $\lambda_1 = -\mu$. Because $\mu > 0$, so that $\lambda_1 < 0$ or in the other hand $|\arg(\lambda_i)| = \pi$. Thus for $0 \leq \alpha < 1$, $|\arg(\lambda_{1,2,3})| > \frac{\alpha\pi}{2}$. The stability of endemic point depends on the fifth order polynomial

$$\lambda^5 + b_1\lambda^4 + b_2\lambda^3 + b_3\lambda^2 + b_4\lambda + b_5 = 0 \quad (12)$$

Based on Theorem 2, The sufficient condition for $n > 3$ is

- $\Delta_1 = b_1 > 0$,
- $\Delta_2 = b_1b_2 - b_3 > 0$ if $b_1b_2 > b_3$,
- $\Delta_3 = b_1b_2b_3 + b_1b_5 - b_1^2b_4 + b_3^2 > 0$, jika $b_1b_2b_3 + b_1b_5 > b_1^2b_4 - b_3^2$,
- $\Delta_4 = 0$.

If all condition is satisfied, then it can be claimed that $|\arg(\lambda_i)| > \frac{\alpha\pi}{2}$ for all $\alpha \in [0,1)$.

4. Parameter Estimation: Case study of COVID-19 cases in Indonesia

We estimated the model parameters using real data. COVID-19 data from Indonesia, spanning August 14, 2021, to September 25, 2021, was used for this purpose. By utilizing optimization tools '*fmincon*' in MATLAB software that find minimum of constrained nonlinear multivariabe function. The estimated parameters were obtained from the active COVID-19 cases in Indonesia, as shown in Figure 2. The results of the parameter estimation, presented in Table 2, will be used in the numerical simulation of model (4).

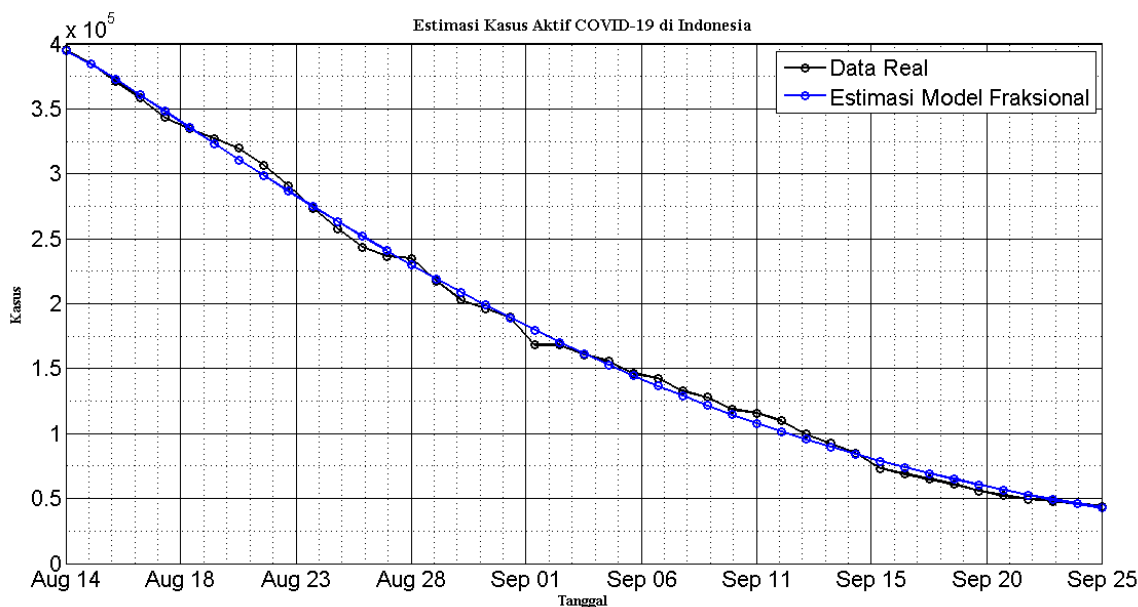


Figure 2. The number of active cases COVID-19 in Indonesia using real data and model for obtaining some parameters.

Table 2. Some parameters value based on real data of COVID-19 in South Sulawesi and Indonesia

Parameter	Value
θ	0.09155
β	0.3079
σ	0.2021
d	0.0870
γ	0.1196
α^*	0.9856

Comparing the approximation using α^* with other values to the real data reveals a smaller relative error than other orders, as shown in Figure 3. Additionally, an error analysis between the fractional model and the real data of active COVID-19 cases in Indonesia is provided in Table 5.

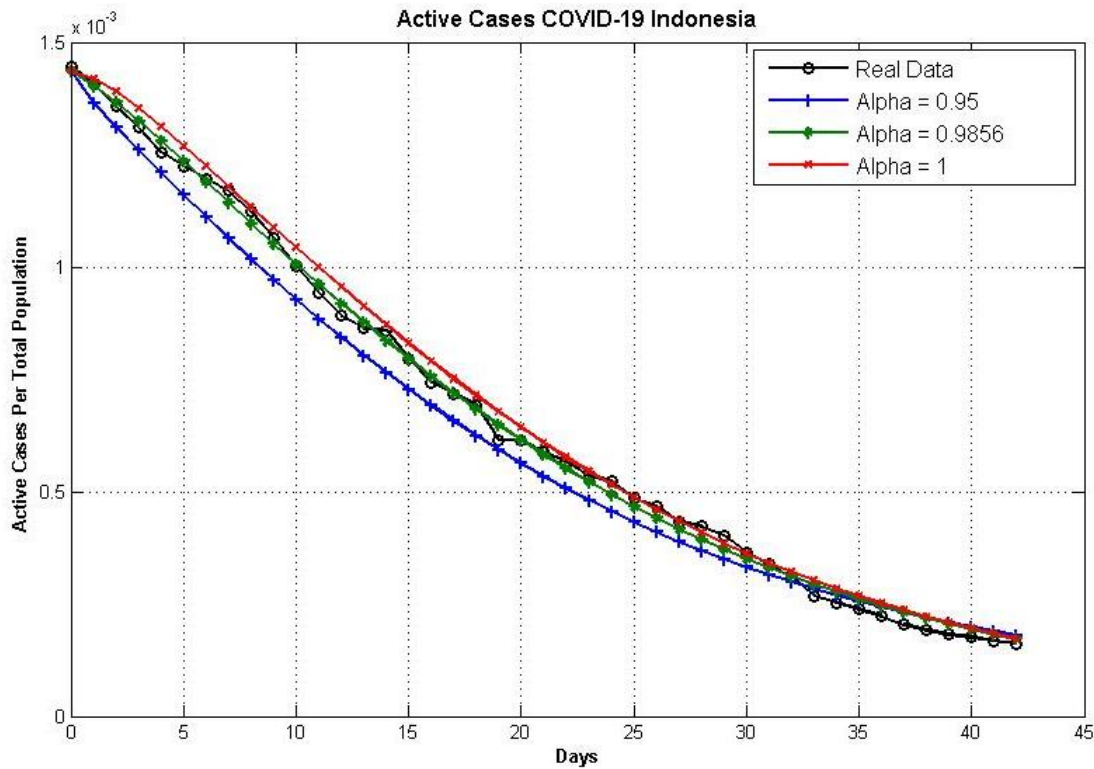


Figure 3. Total active cases of COVID-19 in Indonesia comparing between real data, approximation of estimated order α (green line) and other order.

Table 3. Error Analysis between Fractional Model and Real Data of Active Cases COVID-19 Indonesia

Orde Fraksional	Mean Absolut Deviation	Mean Squared Deviation	Root Mean Square Error	Mean Error Relatif	Mean Absolute Percentage Error
Alpha = 0.95	4.837E-05	2.964E-09	5.444E-05	0.084596487	0.255671528
Alpha = 0.9856	1.685E-05	3.689E-10	1.920E-05	0.042606043	0.159557071
Alpha = 1	2.497E-05	9.097E-10	3.016E-05	0.052266608	0.161091401

When comparing our result with those of Ndairou et al., (2021), we find that different value of α provide better approximation for the real data. The approximation for Indonesia using fractional model yields better results than integer-order model, similar to the findings for Spain ($\alpha = 0.85$) and Portugal ($\alpha = 0.75$), with Indonesia having $\alpha = 0.9856$. Using the estimated parameters, we calculated the basic reproduction number for COVID-19 cases in Indonesia as $R_0 = 0.3925$. This indicates that the spread of COVID-19 has low level in Indonesia and can potentially be reduced within the population.

5. Numerical Simulation and Discussion

Based on the estimated parameters of COVID-19 spread model in Indonesia, the basic reproduction number (R_0) is 0.3925. We consider varying some parameter values to observe their effects on the number of infected cases and the R_0 value.

a. Scenario the change of vaccination rate

From estimated parameter using real data in Indonesia, we obtained a vaccination rate (θ) = 0.0915. Assuming that other parameters remain constant, the following scenarios will occur when value of θ is altered.

Table 4. Scenario of change vaccination rate for model of COVID-19 spread using fractional order in Indonesia

Parameter	Scenario 1	Scenario 2	Scenario 3
$\theta = 0.0915$	0.0915	0.183	0.4575

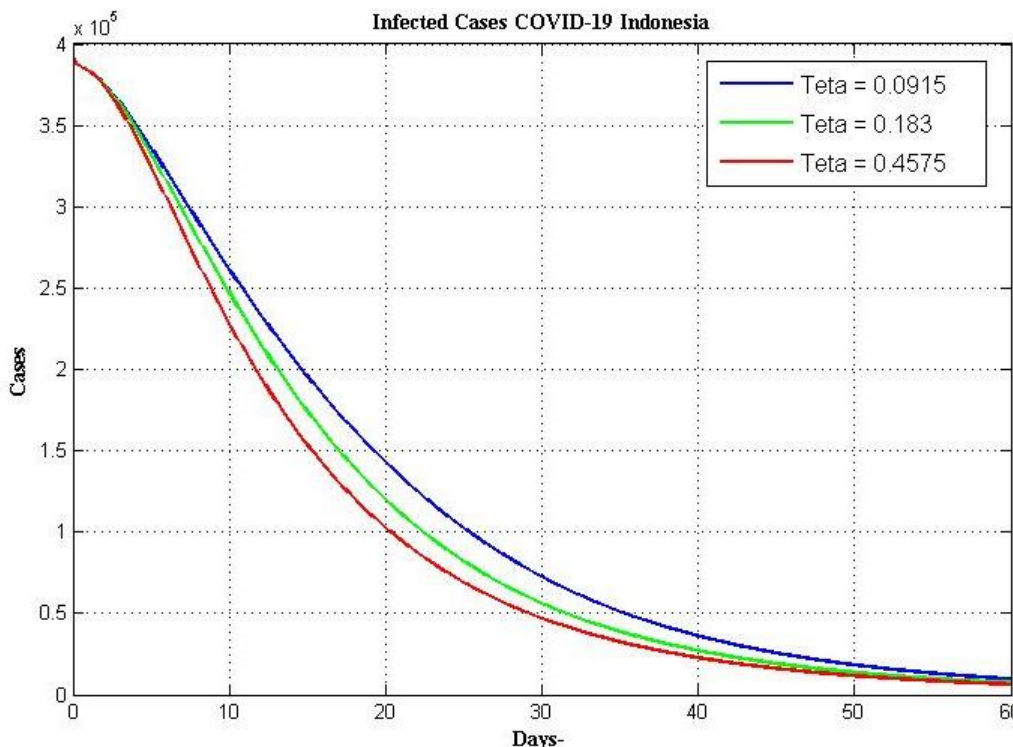


Figure 4. Number of infected cases in Indonesia by performing the change of vaccination rate with $\alpha=0.9856$

Figure 4 illustrates three different scenarios with various values of the vaccination rate θ . The first scenario shows the number of infected cases using the estimated value. In the second scenario, the vaccination rate is increased by 50%, resulting in a faster decrease in the number of infected cases compared to the first scenario. The increase in the vaccination rate for this scenario has a slight impact on the number of infected cases compared to the first scenario. In the final scenario, the vaccination rate is 90% higher, leading to the lowest number of infected cases. Overall, all scenarios have $R_0 < 1$, indicating that the number of infected cases may eventually disappear from the population. Based on the simulation results, an increase in the vaccination rate can be practically interpreted as a rise in the number of individuals receiving the vaccine within the same time period. The higher the vaccination rate, the more significant the impact of this strategy in reducing the number of COVID-19 cases within the population.

b. Scenario the change of vaccine efficacy

Based on the estimated parameters using real data in Indonesia, we assume the efficacy vaccine $\varepsilon = 0.65$. Considering that other parameters remain constant; the following scenarios will occur when value of ε is altered.

Table 5. Scenario of change vaccine efficacy for model of COVID-19 spread using fractional order in Indonesia

Parameter	Scenario 1	Scenario 2	Scenario 3
$\varepsilon = 0.65$	0.65	0.7	0.8

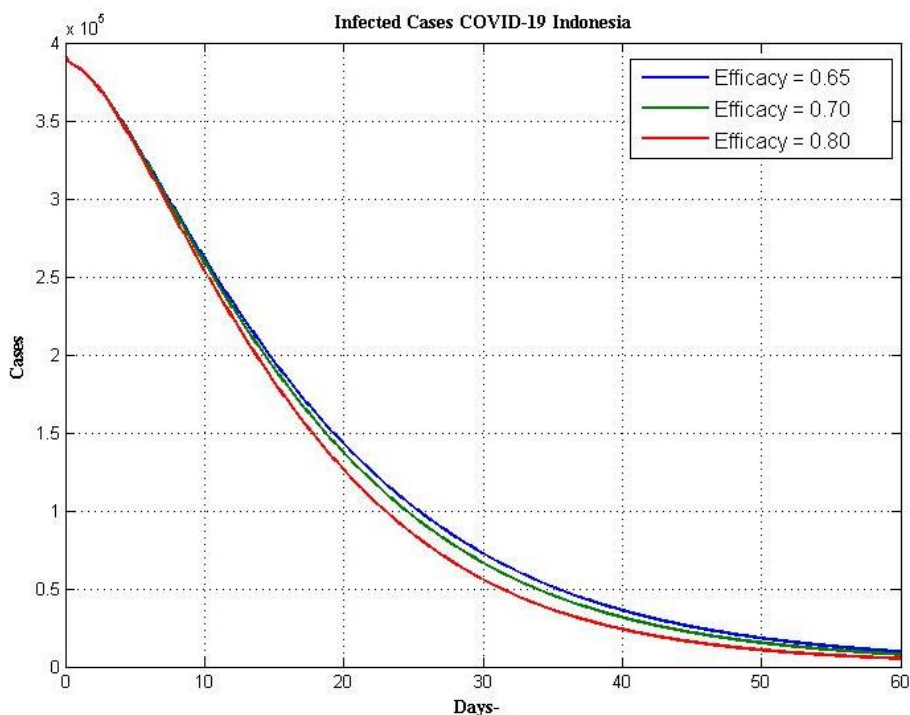


Figure 5. Number of infected cases in Indonesia by performing the change of efficacy vaccine with $\alpha=0.9856$

Figure 5 show the number of infected cases with three scenarios with various value of efficacy ε . In general, if efficacy vaccine is decreased then number of infected cases may increase. All scenarios almost have the same trends each other. In this simulation, we get a slightly different from first to third scenario. Referring to the simulation results, an increase in efficacy can be practically interpreted as the vaccine's ability to provide protection against a specific disease infection. According to these findings, higher efficacy is associated with a reduction in the number of COVID-19 infection cases.

D. CONCLUSION AND SUGGESTIONS

The fractional model gives different value of α to real data of Indonesia. We obtain that $\alpha = 0.9856$ which are well fitted to real data for Indonesia then classical order, according to the result of Error Analysis. The results indicate that the error value in the fractional model is smaller compared to the estimation results for the integer-order model. The simulation also shows that changes of vaccination rate and the efficacy of vaccine give the effect to reduces R_0 . In this study, the researchers assumed that age, infection severity, and population density do not affect disease transmission. Future researchers interested in this topic could conduct studies on COVID-19 that consider age, population density, and infection severity. Further developments can also be achieved by utilizing other numerical methods, such as the Adam-

Bashford Predictor-Corrector Method or the Adomian Laplace Decomposition Method, to obtain more accurate numerical approximations and shorter computational times.

REFERENCES

- Ahmed, E., El-Sayed, A., & El-Saka, H. (2006). On some Routh-Hurwitz conditions for fractional order differential equations and their applications in Lorenz, Rössler, Chua and Chen systems. *Physics Letters A*, 358, 1–4. <https://doi.org/10.1016/j.physleta.2006.04.087>
- Aldila, D., Khoshnaw, S. H. A., Safitri, E., Anwar, Y. R., Bakry, A. R. Q., Samiadji, B. M., Anugerah, D. A., Gh, M. F. A., Ayulani, I. D., & Salim, S. N. (2020). A mathematical study on the spread of COVID-19 considering social distancing and rapid assessment: The case of Jakarta, Indonesia. *Chaos, Solitons & Fractals*, 139, 110042. <https://doi.org/10.1016/j.chaos.2020.110042>
- Annas, S., Isbar Pratama, Muh., Rifandi, Muh., Sanusi, W., & Side, S. (2020). Stability analysis and numerical simulation of SEIR model for pandemic COVID-19 spread in Indonesia. *Chaos, Solitons & Fractals*, 139, 110072. <https://doi.org/10.1016/j.chaos.2020.110072>
- Askar, S. S., Ghosh, D., Santra, P. K., Elsadany, A. A., & Mahapatra, G. S. (2021). A fractional order SITR mathematical model for forecasting of transmission of COVID-19 of India with lockdown effect. *Results in Physics*, 24, 104067. <https://doi.org/10.1016/j.rinp.2021.104067>
- Barros, L. C. de, Lopes, M. M., Pedro, F. S., Esmi, E., Santos, J. P. C. dos, & Sánchez, D. E. (2021). The memory effect on fractional calculus: An application in the spread of COVID-19. *Computational and Applied Mathematics*, 40(3), 72. <https://doi.org/10.1007/s40314-021-01456-z>
- Bas, E., Acay, B., & Ozarslan, R. (2019). Fractional models with singular and non-singular kernels for energy efficient buildings. *Chaos: An Interdisciplinary Journal of Nonlinear Science*, 29(2), 23110. <https://doi.org/10.1063/1.5082390>
- Belgaid, Y., Helal, M., Lakmeche, A., & Venturino, E. (2021). A mathematical study of a coronavirus model with the caputo fractional-order derivative. *Fractal and Fractional*, 5(3). <https://doi.org/10.3390/fractalfract5030087>
- Bernal, J., Gómez-Aguilar, J. F., Cordova, T., Guzman-Cabrera, R., & Rosales, J. (2012). Fractional Mechanical Oscillators. *Revista Mexicana de Física*, 58, 348–352. https://www.researchgate.net/publication/257924332_Fractional_Mechanical_Oscillators
- Carvalho, J. P. S. M. de, & Moreira-Pinto, B. (2021). A fractional-order model for CoViD-19 dynamics with reinfection and the importance of quarantine. *Chaos, Solitons & Fractals*, 151, 111275. <https://doi.org/10.1016/j.chaos.2021.111275>
- Chávez, J., Goetz, T., Siegmund, S., & Wijaya, K. (2017). An SIR-Dengue transmission model with seasonal effects and impulsive control. *Mathematical Biosciences*, 289. <https://doi.org/10.1016/j.mbs.2017.04.005>
- Choi, S., Kang, B., & Koo, N. (2014). Stability for Caputo Fractional Differential Systems. *Abstract and Applied Analysis*, 2014, 1–6. <https://doi.org/10.1155/2014/631419>
- Gómez-Aguilar, J. F., Rosales, J., & Guía, M. (2013). RLC electrical circuit of non-integer order. *Central European Journal of Physics*, 11. <https://doi.org/10.2478/s11534-013-0265-6>
- Iboi, E. A., Ngonghala, C. N., & Gumel, A. B. (2020). Will an imperfect vaccine curtail the COVID-19 pandemic in the U.S.? *Infectious Disease Modelling*, 5, 510–524. <https://doi.org/10.1016/j.idm.2020.07.006>
- Keshtkar, F., Erjaee, G. H., & Boutefnouchet, M. (2014). On stability of equilibrium points in nonlinear fractional differential equations and fractional Hamiltonian systems. *Complexity*, 21. <https://doi.org/10.1002/cplx.21581>
- Müller, S., Kästner, M., Brummund, J., & Ulbricht, V. (2011). A nonlinear fractional viscoelastic material model for polymers. *Computational Materials Science - COMPUT MATER SCI*, 50, 2938–2949. <https://doi.org/10.1016/j.commatsci.2011.05.011>
- Mwalili, S., Kimathi, M., Ojiambo, V., Gathungu, D., & Mbogo, R. (2020). SEIR model for COVID-19 dynamics incorporating the environment and social distancing. *BMC Research Notes*, 13(1), 352. <https://doi.org/10.1186/s13104-020-05192-1>

- Ndairou, F., Area, I., Nieto, J. J., Silva, C. J., & Torres, D. F. M. (2021). Fractional model of COVID-19 applied to Galicia, Spain and Portugal. *Chaos, Solitons & Fractals*, 144, 110652. <https://doi.org/10.1016/j.chaos.2021.110652>
- Ndairou, F., Area, I., Nieto, J., Silva, C., & Torres, D. F. M. (2021). Fractional model of COVID-19 applied to Galicia, Spain and Portugal. *Chaos, Solitons & Fractals*, 144, 110652. <https://doi.org/10.1016/j.chaos.2021.110652>
- Ozalp, N., & Demirci, E. (2011). A fractional order SEIR model with vertical transmission. *Mathematical and Computer Modelling*, 54, 1–6. <https://doi.org/10.1016/j.mcm.2010.12.051>
- Petráš, I. (2011). Fractional Calculus. In I. Petráš (Ed.), *Fractional-Order Nonlinear Systems: Modeling, Analysis and Simulation* (pp. 7–42). Springer Berlin Heidelberg. https://doi.org/10.1007/978-3-642-18101-6_2
- Pimenov, A., Kelly, T. C., Korobeinikov, A., O’Callaghan, M. J. A., Pokrovskii, A. V., & Rachinskii, D. (2012). Memory Effects in Population Dynamics: Spread of Infectious Disease as a Case Study. *Mathematical Modelling of Natural Phenomena*, 7(3), 204–226. <https://doi.org/10.1051/mmnp/20127313>
- Rihan, F. A. (2013). Numerical modeling of fractional-order biological systems. *Abstract and Applied Analysis*, 2013. <https://doi.org/10.1155/2013/816803>
- Saad, K. (2021). Fractal-fractional Brusselator chemical reaction. *Chaos Solitons & Fractals*, 150, 111087. <https://doi.org/10.1016/j.chaos.2021.111087>
- Tang, B. (2020). Dynamics for a fractional-order predator-prey model with group defense. *Scientific Reports*, 10. <https://doi.org/10.1038/s41598-020-61468-3>

Appendix A. Derivation of Sensitivity Analysis

1. Sensitivity Analysis of R_0 with respect to θ

$$C_{\theta}^{R_0} = \frac{\partial R_0}{\partial \theta} \times \frac{\theta}{R_0}$$

$$C_{\theta}^{R_0} = \left[\frac{-\beta p \sigma (bd - bd(1 - \varepsilon))}{d(d + \gamma_1)(d + \sigma)(d + \theta)^2} + \frac{-\beta(1 - p)\sigma(bd - bd(1 - \varepsilon))}{d(d + \gamma_2)(d + \sigma)(d + \theta)^2} \right]$$

$$\times \frac{\theta}{\frac{\beta p \sigma (bd + (1 - \varepsilon)b\theta)}{d(d + \sigma)(d + \gamma_1)(d + \theta)} + \frac{\beta(1 - p)\sigma(bd + (1 - \varepsilon)b\theta)}{d(d + \sigma)(d + \gamma_2)(d + \theta)}}$$

$$C_{\theta}^{R_0} = \left[\frac{-\beta p \sigma b d \varepsilon}{d(d + \gamma_1)(d + \sigma)(d + \theta)^2} + \frac{-\beta(1 - p)\sigma b d \varepsilon}{d(d + \gamma_2)(d + \sigma)(d + \theta)^2} \right]$$

$$\times \frac{\theta}{\frac{\beta p \sigma (bd + (1 - \varepsilon)b\theta)}{d(d + \sigma)(d + \gamma_1)(d + \theta)} + \frac{\beta(1 - p)\sigma(bd + (1 - \varepsilon)b\theta)}{d(d + \sigma)(d + \gamma_2)(d + \theta)}}$$

$$C_{\theta}^{R_0} = \left[\frac{-(d + \gamma_2)\beta p \sigma b d \varepsilon - (d + \gamma_1)\beta(1 - p)\sigma b d \varepsilon}{d(d + \gamma_1)(d + \gamma_2)(d + \sigma)(d + \theta)^2} \right]$$

$$\times \frac{\theta d(d + \sigma)(d + \gamma_2)(d + \gamma_1)(d + \theta)}{\beta p \sigma (d + \gamma_2)(bd + (1 - \varepsilon)b\theta) + \beta(1 - p)\sigma(d + \gamma_1)(bd + (1 - \varepsilon)b\theta)}$$

$$C_{\theta}^{R_0} = \frac{-\beta \sigma b \varepsilon [(d + \gamma_2)p + (d + \gamma_1)(1 - p)]}{(d + \sigma)(d + \theta)}$$

$$\times \frac{\theta d}{\beta \sigma b [p(d + \gamma_2)(d + (1 - \varepsilon)\theta) + (1 - p)(d + \gamma_1)(d + (1 - \varepsilon)\theta)]}$$

$$C_{\theta}^{R_0} = \left[\frac{-\varepsilon((d + \gamma_2)p + (d + \gamma_1)(1 - p))}{(d + \sigma)(d + \theta)} \right] \times \frac{\theta d}{((d + (1 - \varepsilon)\theta)[((d + \gamma_2)p + (d + \gamma_1)(1 - p))])}$$

$$C_{\theta}^{R_0} = \frac{-\varepsilon\theta d}{(d + \sigma)(d + \theta)(d + (1 - \varepsilon)\theta)} < 0$$

2. Sensitivity Analysis of R_0 with respect to ε

$$C_{\varepsilon}^{R_0} = \frac{\partial R_0}{\partial \varepsilon} \times \frac{\varepsilon}{R_0}$$

$$C_{\varepsilon}^{R_0} = \frac{-\beta p \sigma b \theta}{d(d + \sigma)(d + \gamma_1)(d + \theta)} + \frac{-\beta(1 - p)\sigma b \theta}{d(d + \sigma)(d + \gamma_2)(d + \theta)}$$

$$\times \frac{\varepsilon}{\frac{\beta p \sigma (bd + (1 - \varepsilon)b\theta)}{d(d + \sigma)(d + \gamma_1)(d + \theta)} + \frac{\beta(1 - p)\sigma (bd + (1 - \varepsilon)b\theta)}{d(d + \sigma)(d + \gamma_2)(d + \theta)}}$$

$$C_{\varepsilon}^{R_0} = \frac{-\theta \varepsilon}{d + \theta(1 - \varepsilon)} < 0$$